

See discussions, stats, and author profiles for this publication at:
<https://www.researchgate.net/publication/244133655>

A REMPI and ZEKE spectroscopic study of the trans-formanilide·Ar van der Waals cluster

ARTICLE *in* CHEMICAL PHYSICS LETTERS · JANUARY 2002

Impact Factor: 1.9 · DOI: 10.1016/S0009-2614(01)01368-9

CITATIONS

8

READS

18

6 AUTHORS, INCLUDING:



[György Tarczay](#)

Eötvös Loránd University

82 PUBLICATIONS 1,257 CITATIONS

[SEE PROFILE](#)



[Xin Tong](#)

University of Basel

25 PUBLICATIONS 279 CITATIONS

[SEE PROFILE](#)



[Caroline E H Dessent](#)

The University of York

78 PUBLICATIONS 1,483 CITATIONS

[SEE PROFILE](#)

A REMPI and ZEKE spectroscopic study of the *trans*-formanilide · Ar van der Waals cluster

Susanne Ullrich, György Tarczay, Xin Tong, Mark S. Ford, Caroline E.H. Dessent, Klaus Müller-Dethlefs *

Department of Chemistry, University of York, Heslington, York, YO10 5DD, UK

Received 17 September 2001; in final form 14 November 2001

Abstract

Resonance enhanced multiphoton ionization (REMPI) and zero electron kinetic energy (ZEKE) spectra have been obtained for the *trans*-formanilide · Ar (*t*-FA · Ar) cluster. The spectra indicate that the argon atom binds above the aromatic ring to form a C_1 symmetry, van der Waals (vdW) complex. The b_x , b_y and s_z intermolecular vibrational modes are observed at 4, 10 and 18 cm^{-1} in the S_1 state, and 8, 26 and 36 cm^{-1} in the D_0 state. We compare the *t*-FA · Ar spectra with those of other aromatic molecule–argon complexes to probe the electronic structure of FA in the S_1 and D_0 states. © 2002 Published by Elsevier Science B.V.

1. Introduction

There is currently little spectroscopic information available on the *cationic* states of amides [1,2], despite the fact that these states are involved in long-range charge-transfer in polypeptides [3,4]. We have recently employed zero electron kinetic energy (ZEKE) photoelectron spectroscopy to formanilide (FA), a model peptide, with the aim of obtaining basic spectroscopic information to address geometric structure, ionization energies, and *cis*- or *trans*-conformational preference in the FA cation [5,6]. One of the questions that must be addressed when a model system is used to deduce in-

formation on related molecules is how closely the model represents the related molecules. In this context, it is important to explore the extent to which the π -electrons of the FA aromatic ring are delocalized into the amide side chain and vice versa.

In this Letter, we present resonance enhanced multiphoton ionization (REMPI) and ZEKE spectra [7,8] of the *trans*-formanilide · Ar (*t*-FA · Ar) complex, where the argon solvent atom is used as a probe of the electronic structure of the FA solute. By analogy with other aromatic molecule–argon complexes [9–20], *t*-FA · Ar is expected to adopt a van der Waals (vdW) structure where the argon atom binds above the aromatic ring (Fig. 1). The REMPI and ZEKE spectra of *t*-FA · Ar should therefore reflect electronic changes occurring in the aromatic ring in the vicinity of the Ar atom upon $S_1 \leftarrow S_0$ excitation and ionization. We compare the

* Corresponding author. Fax: +44-1904-434527.

E-mail address: kmd6@york.ac.uk (K. Müller-Dethlefs).

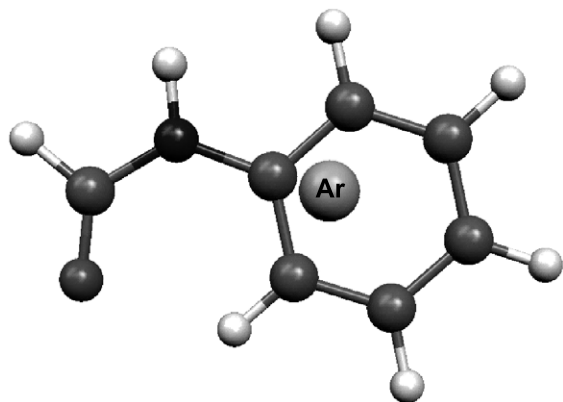


Fig. 1. Schematic diagram of the *t*-FA · Ar vdW complex.

spectra of *t*-FA · Ar with those of other aromatic molecule–argon complexes [9,11–19], to investigate electron-delocalization between the side chain and the aromatic chromophore in FA [21].

In addition to the primary goals of this study described above, *t*-FA · Ar may represent a useful system for further investigating the spectroscopy of the *t*-FA monomer. Observation of *a*'' out-of-plane modes (e.g. torsional modes) in unsolvated *t*-FA, is hampered by the fact that the isomer adopts planar, C_s symmetry conformations in the S_0 , S_1 and D_0 states [6,22,23] so that single-quantum *a*'' excitation is formally forbidden [24]. The REMPI and ZEKE spectra of *t*-FA · Ar may, however, display single-quantum *a*'' vibrational excitation since complexation of *t*-FA with an argon atom is expected to lead to formation of a C_1 symmetry vdW complex (Fig. 1). In addition, the inclusion of the Ar atom may produce an ionization-induced geometry change out of the aromatic plane, and hence improve the Franck–Condon factors (FCFs) for *a*'' vibrational excitation.

2. Experimental

The experimental setup has been described in detail elsewhere [23] and will be discussed only briefly here. FA · Ar clusters were produced in a supersonic jet expansion of FA vapor seeded in an argon/neon mixture (5% argon) from a heated reservoir (140 °C). The reservoir was located immediately behind the pulsed nozzle (general valve,

0.8 mm). Laser wavelengths were calibrated by simultaneously recording iodine spectra with all quoted laser photon energies having been converted from air to vacuum. The pulse sequences, timings and field strengths used to obtain the spectra are identical to those in [25].

3. Results and discussions

3.1. REMPI spectroscopy of *t*-FA · Ar

Fig. 2 displays the two-color ($1 + 1'$) REMPI spectrum of *t*-FA · Ar, recorded with the ioniza-

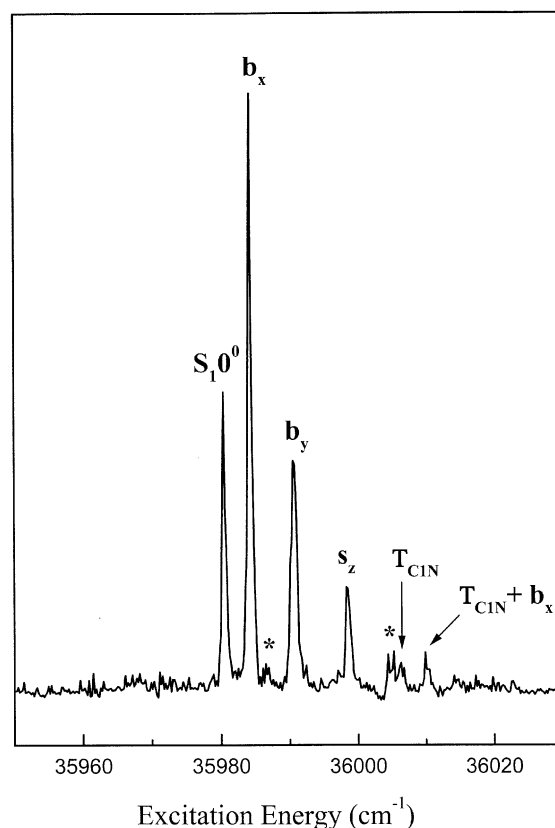


Fig. 2. Two-color ($1 + 1'$) $S_1 \leftarrow S_0$ REMPI spectrum of *t*-FA · Ar, recorded with the ionization laser set to 31496 cm^{-1} . Assignments of the b_x bend, the b_y bend, the intermolecular stretch, s_z , and the T_{CIN} intramolecular torsion are included on the spectrum. Spectral features labelled * are dependent on source conditions, and assigned to fragmentation of higher mass clusters.

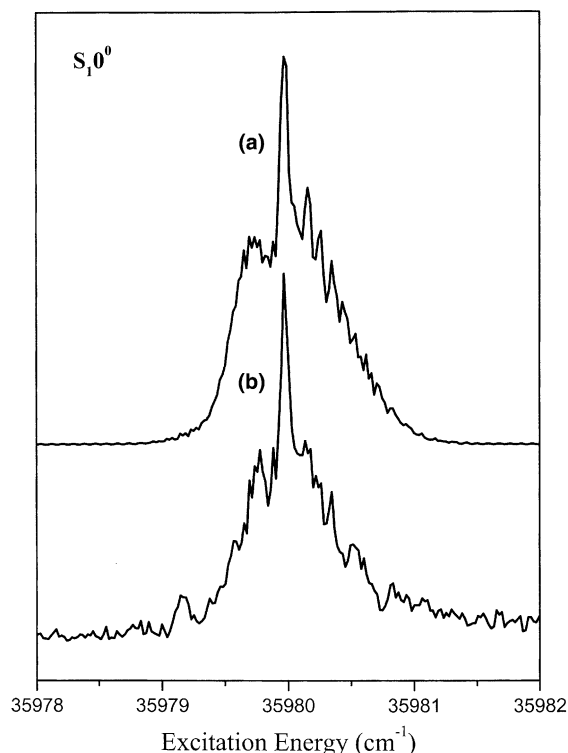


Fig. 3. (a) Simulated band contour for the $S_1 0^0$ transition using fitted rotational constants. The rotation of the transition moment to give a c-type band contour is consistent with a geometric structure where the Ar atom binds above the aromatic ring. (b) Two-color $(1 + 1')$ REMPI spectrum of the $S_1 0^0$ state transition of t -FA · Ar, recorded at higher resolution than the spectrum presented in Fig. 2.

Table 1
Fitted rotational constants (in MHz) for the S_0 and S_1 states of t -FA · Ar

State	<i>A</i>	<i>B</i>	<i>C</i>
S_0	922.5 (1.0)	708.12 (86)	586.61 (70)
S_1	991.0 (1.1)	746.67 (86)	510.92 (62)

Table 2
Frequencies and assignments of the vibrational bands observed in the REMPI spectrum of t -FA · Ar^a

Frequency (cm ⁻¹)	Assignment	Frequency (cm ⁻¹)	Assignment
0	$S_1 0^0$	29	$T_{\text{CIN}} + b_x$
4	b_x	63	B_N
10	b_y	195	B'
18	s_z	199	$B' + b_x$
25	T_{CIN}	—	—

^a The frequencies are given relative to the $S_1 0^0$ origin.

tion laser set to 31496 cm^{-1} . The $S_1 0^0$ origin of the complex appears at $35980.0 \pm 0.2 \text{ cm}^{-1}$, which represents a 24 cm^{-1} red-shift compared to the t -FA monomer [5,6]. This red-shift is similar to those of other aromatic molecule–Ar complexes [9,11–17] which have been shown to adopt vdW structures, and indicates that a similar structure occurs in t -FA · Ar. A higher-resolution REMPI spectrum of the $S_1 0^0$ band of t -FA · Ar is shown with a simulation in Fig. 3. The simulation was made using the fitted rotational constants presented in Table 1. The fitted rotational constants, and the fact that the band contour in Fig. 3 displays some c-type structure, are both consistent with the Ar atom binding above the aromatic ring in the S_0 and S_1 states [26–28].

Several prominent vibrational features are evident in the region above the S_1 origin, which may represent intermolecular vibrations or low-frequency intramolecular modes of FA. Table 2 lists the frequencies of the REMPI spectral features. Of the three possible intermolecular vibrations, we anticipate that the b_x bend (along the B -axis of the complex) should appear more intensely than the b_y bend (C -axis) as a significant geometry change is only expected along the B -axis, towards the side chain. The s_z intermolecular stretch (A -axis) is expected to occur at higher frequency than either b_x or b_y [9,12,13,15]. We therefore assign the features at 4, 10 and 18 cm^{-1} to the b_x bend, the b_y bend, and the s_z intermolecular stretch, respectively.

The feature at 25 cm^{-1} is tentatively assigned as the intramolecular $\text{C}_{\text{ring}}\text{--N}_{\text{amide}}$ torsion, T_{CIN} , which displays a fundamental frequency of $\sim 35 \text{ cm}^{-1}$ in the monomer [6]. Single-quanta excitation of T_{CIN} was not evident in the monomer spectrum,

but appears in the spectrum of the complex due to the relaxation of symmetry. The intramolecular bending mode centered on the nitrogen atom, B_N [6] was observed at 63 cm^{-1} . An additional feature at 195 cm^{-1} (not displayed in Fig. 2 to enhance the presentation of the origin region) is assigned to the in-plane side-arm bend, B' , which is found at 196 cm^{-1} in the monomer [6]. No additional features were observed scanning as far as 36400 cm^{-1} , and there appears to be no prominent excitation of the amide torsion upon $S_1 \leftarrow S_0$ excitation.

The b_x bend is the dominant spectral feature in the $t\text{-FA} \cdot \text{Ar}$ REMPI spectrum; this contrasts with those of other aromatic molecule–argon complexes, such as fluorobenzene $\cdot \text{Ar}$ [9] and phenol $\cdot \text{Ar}$ [15] where the origin transitions dominate the spectra. Thus, the $t\text{-FA} \cdot \text{Ar}$ REMPI spectrum indicates a relatively large geometry change for the vdW complex compared with similar argon complexes; this maximizes the FCFs for the $S_1 b_x \leftarrow S_0 0^0$ transition. The geometry change can be attributed to a considerable shift of π -electron density towards the $\text{C}_{\text{ring}}\text{--N}_{\text{amide}}$ bond within the monomer upon excitation, thus significantly changing the potential experienced by the argon atom. Complimentary information with respect to changes in electron density is presented in a study of $t\text{-FA} \cdot \text{H}_2\text{O}$ [29]. We note that despite the strength of the $S_1 b_x \leftarrow S_0 0^0$ transition, no b_x overtones are evident. The prominent excitation of the b_y bend also reflects the substantial change in electron-delocalization within the side chain upon excitation.

It is notable that the frequencies of the intermolecular modes observed in the $t\text{-FA} \cdot \text{Ar}$ REMPI spectrum are considerably lower than in comparable systems [9,12,13,15]. For example, the b_x and s_z vibrations appear at 4 and 18 cm^{-1} , respectively, in the S_1 state of $t\text{-FA} \cdot \text{Ar}$ while the corresponding frequencies in the S_1 state spectrum of the phenol $\cdot \text{Ar}$ complex are 20 and 45 cm^{-1} [15]. The low frequency intermolecular vibrations of $t\text{-FA} \cdot \text{Ar}$ reflect the comparatively weak intermolecular bond, which can be attributed to the increased conjugation of the aromatic π -electrons into the amide side chain in the S_1 excited state. This counterbalances the increase in π -electron

polarizability that generally accompanies $S_1 \leftarrow S_0$ excitation, so that the strength of the aromatic–argon bond is reduced overall. The b_x frequency is particularly low, an indication that substantial electron density is located along the $\text{C}_{\text{ring}}\text{--N}_{\text{amide}}$ bond, softening the S_1 state potential along this coordinate.

3.2. ZEKE spectroscopy of $t\text{-FA} \cdot \text{Ar}$

Fig. 4a displays the $(1+1')$ ZEKE spectrum of the $t\text{-FA} \cdot \text{Ar}$ cluster recorded via the $S_1 0^0$ intermediate state. The lowest energy feature at $67238 \pm 5\text{ cm}^{-1}$ is assigned as the ionization energy (IE), which is red-shifted by 169 cm^{-1} compared to the bare monomer transition [5,6]. This

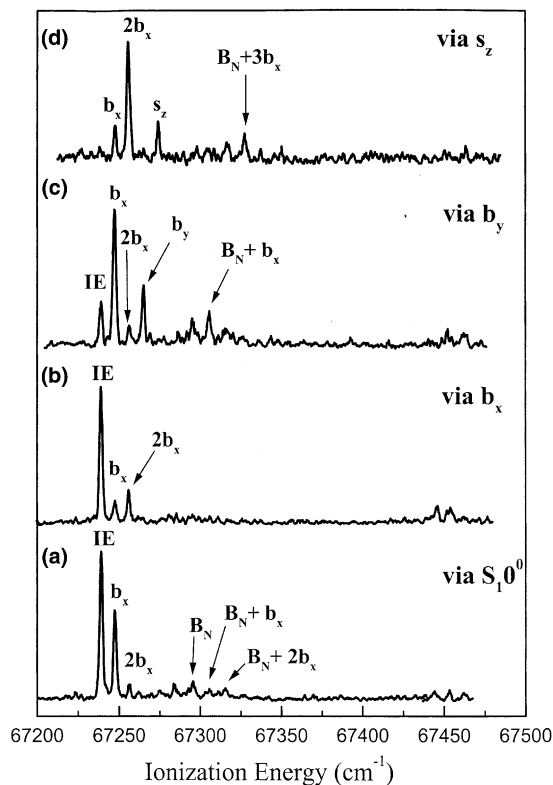


Fig. 4. ZEKE spectra of $t\text{-FA} \cdot \text{Ar}$ recorded via: (a) $S_1 0^0$; (b) $S_1 b_x$; (c) $S_1 b_y$; (d) $S_1 s_z$. Assignments of the b_x bend, the b_y bend, the intermolecular stretch, s_z , and the B_N intramolecular bend are included on the spectrum.

IE red-shift is comparable to those of other aromatic molecule–Ar complexes [9,11,14–18] in line with a cationic vdW structure. While this geometric structure is clearly a local minimum for *t*-FA · Ar, it may not represent the minimum energy D_0 state structure. The ZEKE spectrum of phenol · Ar⁺ similarly revealed the existence of an above ring complex [15] although the global minimum was subsequently shown to correspond to a hydrogen-bonded structure [30].

The IE feature is the most intense band in the *t*-FA · Ar ZEKE spectrum recorded via the S_10^0 state, indicating that a relatively modest geometric change occurs between the S_1 and D_0 states. A number of low frequency vibrational features are evident in the region above the IE at 8, 17, 23, 36, 45, 57, 67, 77, 204 and 214 cm^{−1}. The features at 8 and 17 cm^{−1} are assigned to the b_x bend by comparison with the ZEKE spectra of other aromatic molecule–Ar complexes, e.g., fluorobenzene · Ar [9] and phenol · Ar [15], where dominant progressions of this mode are observed. We note that the b_x progression extends to only two quanta in the *t*-FA · Ar ZEKE spectrum whereas at least three quanta are evident in the fluorobenzene · Ar and phenol · Ar spectra, with the b_x feature representing the most intense spectral band. This reveals that the $D_0 \leftarrow S_1$ geometry change in *t*-FA · Ar is smaller than in other argon–aromatic molecule complexes [9,11,14–18] possibly due to the electron

density shifting from the side chain to the aromatic ring upon ionization, leading to similar S_1 and D_0 state structures.

The feature at 57 cm^{−1} is assigned to, B_N , which appears at 68 cm^{−1} in the bare monomer [6]. A b_x combination progression is built off this mode, with a spacing of 10 cm^{−1}, indicating that the Ar atom is slightly more strongly bound along the b_x coordinate when B_N is excited. The features at 204 and 214 cm^{−1} are assigned to the B' intramolecular mode (the in-plane side-arm bend which appears at 211 cm^{−1} in the monomer [5,6]) plus its combination with b_x .

Fig. 4b displays the *t*-FA · Ar ZEKE spectrum recorded via the S_1b_x intermediate state. In line with the propensity rule [8] the FCFs of the b_x progression are modified in this spectrum compared to the spectrum obtained via the S_1 origin, confirming that the 8 cm^{−1} mode in the ion corresponds to the 4 cm^{−1} mode in the S_1 state. Although the B' and $B' + b_x$ features are again visible, there is little additional vibrational structure in this spectrum.

Fig. 4c displays the spectrum obtained via the S_1b_y intermediate state, where the FC envelope is extended to higher ion internal energy than in the spectra presented in Fig. 4a,b. A feature is visible at 26 cm^{−1} ion internal energy, which was absent from the spectra recorded via the S_10^0 and S_1b_x states, and is assigned as the cationic b_y mode on

Table 3

Frequencies (cm^{−1}) and assignments of the vibrational bands observed in the ZEKE spectra of *t*-FA · Ar^a

Assignment	Via 0^0	Via b_x	Via b_y	Via s_z
b_x	8	8	8	9
$2b_x$	17	17	17	17
T_{CIN}	23	—	—	—
b_y	—	—	26	—
s_z	36	—	—	36
$s_z + b_x$ or $2T_{CIN}$	45	—	—	—
B_N	57	—	57	—
$B_N + b_x$	67	—	67	—
$B_N + 2b_x$	77	—	77	77
$B_N + 3b_x$	—	—	87	88
$B_N + 4b_x$	—	—	97	98
$B_N + 5b_x$	—	—	—	108
B'	204	206	205	—
$B' + b_x$	214	215	214	—

^a The frequencies are given relative to the ionization energy.

the basis of the propensity rule. The absence of the b_y vibration in the spectrum recorded via the $S_1 0^0$ state indicates that there is little change in the electronic structure of *t*-FA along the b_y coordinate upon ionization.

Finally, the spectrum recorded via the $S_1 s_z$ intermediate state is presented in Fig. 4d. The spectral feature at 36 cm^{-1} , is not prominent in the other ZEKE spectra, and is assigned to the s_z intermolecular stretch. This pattern reflects the one found in the phenol \cdot Ar ZEKE spectra where s_z is only clearly observed in the ZEKE spectrum recorded via the $S_1 s_z$ state [15]. In the spectrum recorded via $S_1 0^0$, the feature at 36 cm^{-1} ion internal energy can now also be assigned to s_z , suggesting that the feature at 45 cm^{-1} represents the $s_z + b_x$ combination. This assignment seems unlikely, however, given that the 45 cm^{-1} feature is more intense than the s_z band. Alternatively, the 45 cm^{-1} feature could represent two quanta excitation of the rather weak feature found at 23 cm^{-1} , which is tentatively assigned to T_{CIN} (33 cm^{-1} in the monomer [6]). The spectral features observed in the ZEKE spectra of *t*-FA \cdot Ar are listed in Table 3 with suggested assignments.

It is of interest to compare the frequencies of the intermolecular modes observed in the *t*-FA \cdot Ar ZEKE spectra to those of other aromatic molecule–Ar complexes. In the D_0 states of phenol \cdot Ar and fluorobenzene \cdot Ar, the b_x vibrations appear at 15 and 20 cm^{-1} , respectively, while the s_z vibrations appear at 66 and 43 cm^{-1} , indicating that the argon atom in *t*-FA \cdot Ar is comparatively more weakly bound. This is a direct reflection of the delocalization of electron density from the amide side chain to the aromatic ring in the cation [21] in line with the results of ab initio calculations of FA^+ [6].

4. Summary

The REMPI and ZEKE spectra of *t*-FA \cdot Ar reveal that the b_x , b_y and s_z intermolecular vibrations occur at 4, 10 and 18 cm^{-1} , respectively, in the S_1 state and at 8, 26, 36 cm^{-1} , in the D_0 state. The increased frequencies of these modes in the D_0 state reflects the strengthening of the intermolec-

ular bond that occurs due to the additional charge-induced dipole interaction in *t*-FA \cdot Ar^+ . In general, the intermolecular modes in both the S_1 and D_0 states display lower frequencies than in other aromatic molecule–Ar complexes. This effect is interpreted in terms of increased conjugation of the π -electrons with the amide side chain, and to excess charge delocalization into the side chain in the cation reducing the charge-induced dipole interaction. In turn, this implies that the side chain possess some cationic character in the D_0 state of *t*-FA making *t*-FA $^+$ a useful model system for studying the properties of cationic amides. The Ar atom in the FA \cdot Ar complex studied here primarily probes the FA solute in the vicinity of its binding site, the aromatic ring. However, the study of other molecular complexes, such as FA \cdot H_2O [29] can provide information on the electronic structure of the amide side chain of FA.

Acknowledgements

We thank the EPSRC for financial support (Chemistry GR/L27770) of this work. S.U. acknowledges support from the Fonds des Verbandes der Chemischen Industrie and a DAAD Doktorandenstipendium. G.T. thanks the Hungarian Ministry of Education for a Eötvös Scholarship, and the Peregrinatio II Foundation for further support. C.E.H.D. thanks the Royal Society for support from a University Research Fellowship.

References

- [1] V.V. Zverev, *Izv. Akad. Nauk SSR, Ser. Kim.* 3 (1992) 602.
- [2] E.G. Robertson, M.R. Hockridge, P.D. Jeffs, J.P. Simons, *Phys. Chem. Chem. Phys.* 3 (2001) 786.
- [3] E.W. Schlag, S.Y. Sheu, D.Y. Yang, H.L. Selzle, S.H. Lin, *Proc. Natl. Acad. Sci.* 97 (2000) 1068.
- [4] S.Y. Sheu, E.W. Schlag, D.Y. Yang, H.L. Selzle, *J. Phys. Chem. A* 105 (2001) 6353.
- [5] S. Ullrich, G. Tarczay, X. Tong, C.E.H. Dessent, K. Müller-Dethlefs, *Ang. Chemie. Int. Ed.* (in press).
- [6] S. Ullrich, G. Tarczay, X. Tong, C.E.H. Dessent, K. Müller-Dethlefs, *Phys. Chem. Chem. Phys.* (in press).
- [7] C.E.H. Dessent, K. Müller-Dethlefs, *Chem. Rev.* 100 (2000) 3999.

- [8] K. Müller-Dethlefs, E.W. Schlag, *Ang. Chem. Int. Ed.* 37 (1998) 1346.
- [9] G. Lembach, B. Brutschy, *J. Chem. Phys.* 107 (1997) 6156.
- [10] H. Krause, H.J. Neusser, *Chem. Rev.* 94 (1994) 1829.
- [11] K. Kimura, *J. Electron Spectrosc.* 108 (2000) 31, and references therein.
- [12] E.J. Bieske, M.W. Rainbird, I.M. Atkinson, A.E.W. Knight, *J. Chem. Phys.* 91 (1989) 752.
- [13] M. Mons, J.L. Calve, F. Piuze, I. Dimicoli, *J. Chem. Phys.* 92 (1990) 2155.
- [14] X. Zhang, J.L. Knee, *Faraday Discuss.* 97 (1994) 299.
- [15] S.R. Haines, C.E.H. Dessent, K. Müller-Dethlefs, *J. Electron Spectrosc. Rel. Phenom.* 108 (2000) 1.
- [16] C.E.H. Dessent, S.R. Haines, K. Müller-Dethlefs, *Chem. Phys. Lett.* 315 (1999) 103.
- [17] L.A. Chewter, K. Müller-Dethlefs, E.W. Schlag, *Chem. Phys. Lett.* 135 (1987) 219.
- [18] M.C.R. Cockett, K. Kimura, *J. Chem. Phys.* 100 (1994) 3429.
- [19] D. Bahatt, A. Heidenreich, N. Benhorin, U. Even, J. Jortner, *J. Chem. Phys.* 100 (1994) 6290.
- [20] H. Piest, G. Von Helden, G. Maier, *J. Chem. Phys.* 111 (1999) 10750.
- [21] M.D. Patey, C.E.H. Dessent, *J. Phys. Chem. A.* (submitted).
- [22] J.A. Dickinson, M.R. Hockridge, E.G. Robertson, J.P. Simons, *J. Phys. Chem. A* 103 (1999) 6938.
- [23] E.G. Robertson, *Chem. Phys. Lett.* 325 (2000) 299.
- [24] P.R. Bunker, P. Jensen, *Molecular Symmetry and Spectroscopy*, second ed., NRC, Ottawa, 1998.
- [25] S.R. Haines, W.D. Geppert, D.M. Chapman, M. Watkins, C.E.H. Dessent, M.C.R. Cockett, K. Müller-Dethlefs, *J. Chem. Phys.* 109 (1998) 9249.
- [26] M.S. Ford, S.R. Haines, I. Pugliesi, C.E.H. Dessent, K. Müller-Dethlefs, *J. Electron Spectrosc. Rel. Phenom.* 112 (2000) 231.
- [27] A. Bacon, J.M. Hollas, *Faraday Discuss. Chem. Soc.* 86 (1988) 129.
- [28] B.D. Howells, J. McCombie, T.F. Palmer, J.P. Simons, A. Walters, *J. Chem. Soc. Faraday Trans* 88 (1992) 2603.
- [29] S. Ullrich, G. Tarczay, X. Tong, C.E.H. Dessent, K. Müller-Dethlefs, *Phys. Chem. Chem. Phys.* (in preparation).
- [30] N. Scola, O. Dopfer, *J. Mol. Struct.* 563 (2001) 241.